JOURNAL OF CATALYSIS **159,** 305–312 (1996)
ARTICLE NO. 0092

Oxidation of Adsorbed CH_3 and C_2H_5 Species on Rh(111)[1]

L. Bugyi, A. Oszkó, and F. Solymosi

Institute of Solid State and Radiochemistry, A. József University and Reaction Kinetics Research Group of the Hungarian Academy of Sciences, P.O. Box 168, H-6701 Szeged, Hungary

Received July 11, 1995; revised November 7, 1995; accepted November 24, 1995

The reaction pathways of adsorbed CH_3 and C_2H_5 in the presence of coadsorbed oxygen atoms on the Rh(111) surface were investigated by means of temperature-programmed desorption (TPD), X-ray photoelectron spectroscopy (XPS), and high-resolution electron energy loss spectroscopy (HREELS). CH_x fragments were produced by the dissociation of the corresponding iodo compounds. Oxygen adatoms significantly stabilized carbon–iodide bonds and induced the desorption of strongly adsorbed methyl and ethyl iodides. A weak signal of methoxy species has been detected by HREELS in the low temperature interaction of CH_3 and O. Oxidation of hydrocarbon fragments led to the production of H_2O, CO, and CO_2 above 350 K. In the case of the adsorbed ethyl species, the formation of gaseous acetaldehyde was also established. It is assumed that the oxidation of CH_x fragments proceeds through the transient formation and reactions of adsorbed methoxy and ethoxy species, preceded by the interaction of methyl and ethyl groups of adsorbed iodo compounds with the adsorbed oxygen atoms.

1. INTRODUCTION

Rhodium-based materials are among the most effective catalysts in the synthesis of hydrocarbons and oxygenated compounds (1–5), in the $CH_4 + CO_2$ reaction (6–8), and in the dehydrogenation of CH_4 under nonoxidative conditions (9, 10). For the elucidation of elementary steps in these reactions it is of primary importance to evaluate the chemistry of hydrocarbon fragments (CH_2, CH_3, C_2H_5) transitorily formed on the Rh surface in the catalytic processes. As a first step in this direction we generated hydrocarbon fragments on Rh(111) by thermal and photodissociation of the corresponding iodo compounds and determined their thermal stability and reaction pathways (11–13). Recently, this program was extended to oxygen-covered Rh(111), where selective oxygen addition to adsorbed CH_2 species was observed to yield gaseous CH_2O (12, 14). In the present paper we report on the reactions of CH_3 and C_2H_5 with adsorbed oxygen atoms on the Rh(111) surface.

[1] A part of this paper was presented at the 14th North American Meeting of the Catalysis Society, June 11–16, 1995.

2. EXPERIMENTAL

The Rh crystal used in this work was cut from a single-crystal boule (Materials Research Corporation, purity 99.99%). Initially the sample was cleaned by cycled heating in oxygen. This was followed by cycles of argon-ion bombardment (typically 1–2 kV, 1×10^{-6} Torr Ar, 1000 K, 3 μA for 10–30 min) and annealing at 1270 K for several minutes. CH_3I and C_2H_5I were products of Merck. They were degassed and purified by freeze–pump–thaw cycles.

The experiments were performed in two separate UHV chambers with a routine base pressure of 2×10^{-10} Torr produced by turbomolecular, ion-getter, and titanium sublimation pumps. One chamber was equipped with facilities for Auger electron spectroscopy (AES), high resolution electron energy loss spectroscopy (HREELS) and temperature-programmed desorption (TPD). The HREEL spectrometer (VSW, type HA-50) was situated in the lower level of the chamber and has a resolution of 70–100 cm^{-1}. All energy loss spectra were recorded with a primary electron energy of 5.0 eV and at an incident angle of 45°. The second system was a Kratos XSAM 800 instrument, where X-ray photoelectron spectroscopy (XPS) measurements were performed using Mg$K\alpha$ radiation (14 kV, 10 mA). All binding energies are referred to the Fermi level of the Rh($3d_{5/2}$), which places the Rh($3d_{5/2}$) photoelectron line at 307.2 eV. The pass energy of the electron energy analyzer was set to 40 eV, which gives a full width at half maximum (FWHM) of 1.65 eV for the Rh($3d_{5/2}$) photoelectron line for a clean Rh(111) surface. Collection times for XPS were 15 and 30 min, respectively. The heating rate for TPD measurements was ca. 20 K/s. Further experimental details have been described elsewhere (12).

The adsorption of oxygen was performed at 300 K, while that of iodo compounds was carried out at 90 K. Gases were dosed through a 0.1 mm diameter capillary that terminated 2 cm from the sample. The local pressure at the sample was about 10^{-7} Torr during dosing. According to previous measurements the surface concentration of oxygen on Rh(111) at saturation corresponds to 0.5 monolayer, $\Theta_O = 0.5$ (15, 16). The LEED pattern observed is attributed to three domains of $p(2 \times 1)$–O (16).

0021-9517/96 $18.00

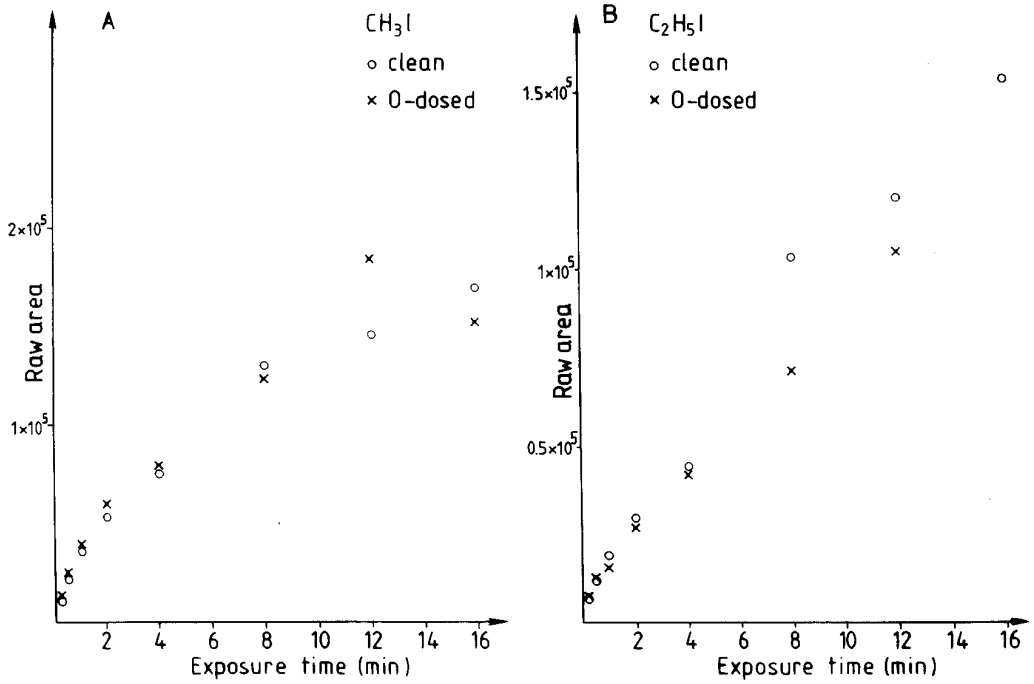

FIG. 1. Areas of the I($3d_{5/2}$) peak in the XP spectra on Rh(111) as a function of (A) CH_3I exposure and (B) C_2H_5I exposure at 90 K on clean (○) and oxygen-dosed (x) ($\Theta_O = 0.4$) surface.

3. RESULTS

3.1. Reaction of CH_3I and CH_3 Species

Previous studies clearly demonstrated that XPS is a suitable method for following the dissociation of iodo compounds on metal surfaces, as the binding energy of I($3d_{5/2}$) in the atomically adsorbed state is about 1.0–1.5 eV lower than that for molecularly adsorbed iodo compounds (17–19). Following the adsorption of CH_3I on a clean Rh(111) surface at 90 K, the binding energy of I($3d_{5/2}$) appeared at 620.3 eV and that of C(1*s*) at 284.9 eV. The positions of the peaks were practically independent of the coverage. The same features were observed for oxygen-dosed Rh(111) at $\Theta_O = 0.4$. In Fig. 1A the areas of the I($3d_{5/2}$) peak were plotted as a function of CH_3I exposure. We found that the uptake of CH_3I is almost the same for both surfaces.

XP spectra of adsorbed layers annealed at different temperatures are presented in Fig. 2. Whereas on the clean surface a shift in the binding energy of adsorbed I began to occur at 175 K and was complete at 200 K; on an oxygen-dosed surface these changes were observed at higher temperatures 225–275 K. The intensity of the I($3d_{5/2}$) peak remained

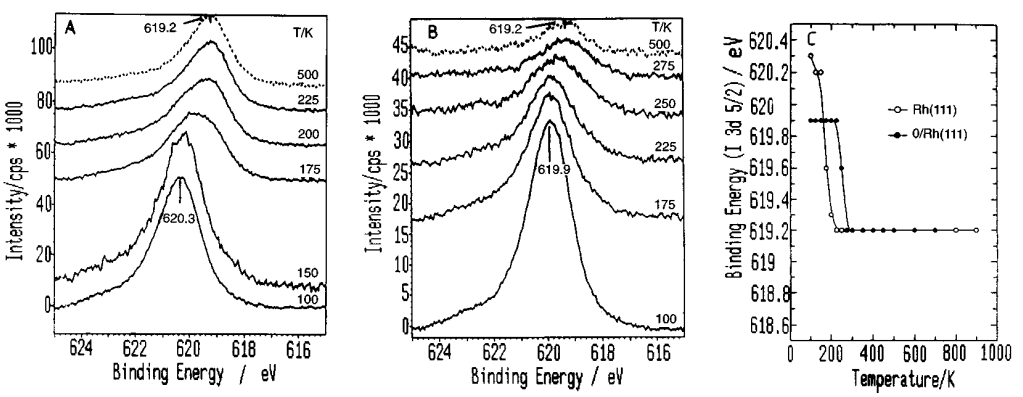

FIG. 2. Effects of annealing on the I($3d_{5/2}$) XP spectra of adsorbed CH_3I on (A) clean Rh(111) and (B) oxygen-dosed Rh(111) ($\Theta_O = 0.4$) and (C) on the position of the I($3d_{5/2}$) peak. The exposure time of CH_3I was 8 min.

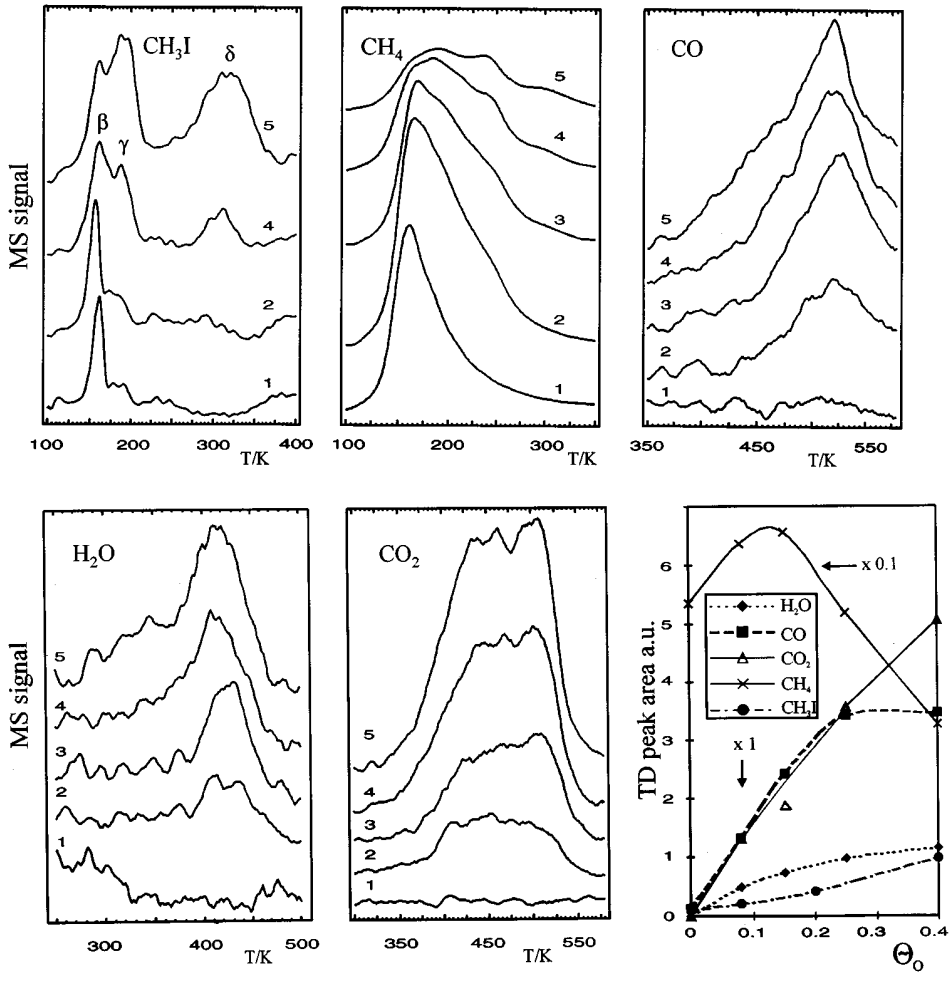

FIG. 3. TPD profiles of various products following CH_3I adsorption at 90 K on oxygen-dosed Rh(111) at different oxygen coverages and the areas of TPD peaks of the desorption products as a function of oxygen coverage. The exposure time of CH_3I was 4 min. The values of oxygen coverages Θ_O: (1) 0.00; (2) 0.08; (3) 0.15; (4) 0.20; (5) 0.40.

unaltered in the temperature range of 400–700 K. The peak was completely eliminated only at around 1100 K. This is in accord with the results of AES measurements (11).

Previous studies on the clean surface showed that in TPD experiments the molecularly adsorbed CH_3I desorbs to give two peaks, $T_p = 160$ K (β) and 136 K (α) (11). The latter was ascribed to a multilayer as it could not be saturated. TPD profiles presented in Fig. 3 reveal that in the presence of preadsorbed oxygen the picture is more complex. At higher oxygen coverages, a fraction of the CH_3I desorbs in new desorption states (denoted by γ and δ) with $T_p = 180$ and 320 K, in addition to the α and β peaks. At saturation oxygen coverage, the amount of CH_3I desorbing in the peak δ ($T_p = 320$ K) exceeds that desorbing in the other peaks. No desorption of other I-containing compounds was observed below 700 K. Methane is also formed on oxygen-covered Rh: after a transitory increase its amount decreased with the increase of oxygen coverage, and its peak temperature shifted from 160 K to 185 and 240 K.

The formation of new products, CO_2 ($T_p = 450$ and 500 K), CO ($T_p = 520$ K), and H_2O ($T_p = 415$ K) suggests that CH_3 undergoes oxidation between 400 and 500 K. The products of oxidation gradually increase in amount with the oxygen coverage. Note that CH_2O has not been identified in the desorbing products. An attempt was also made to detect CH_3OH, C_2H_6, and C_2H_4 without any positive result. Analysis of TPD results shows that at $\Theta_O = 0.4$ about 77% of the CH_3 species have been oxidized and 23% have been converted into CH_4.

In a search for surface intermediates in the oxidation reaction, HREELS measurements were carried out under similar conditions. Spectra are displayed in Fig. 4. The losses obtained for O-covered Rh(111) corresponded well to the molecularly adsorbed CH_3I. The characteristic losses of adsorbed CH_3I, CH_3, and CH_3O on the Rh(111) surface, together with their assignments, are listed in Table 1.

On warming the adsorbed layer to 150–180 K, a new loss feature appeared at 1040–1050 cm^{-1}, which was eliminated

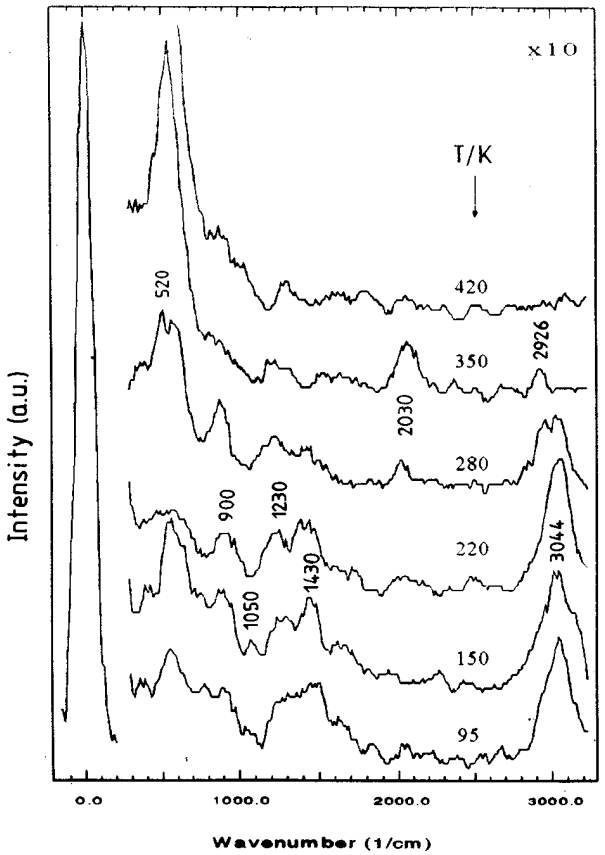

FIG. 4. HREEL spectra of absorbed CH_3I on oxygen-covered Rh(111) ($\Theta_O = 0.4$) after annealing at different temperatures. The exposure time of CH_3I was 4 min.

at 185–200 K. Further changes occurred above 220 K: the losses of adsorbed CH_3I attenuated, and new losses developed at 2920–2930, 2020–2030, and 520 cm^{-1}. At 310–350 K the dominant losses were at 2926 and 2040–2050 cm^{-1}. The loss at 520 cm^{-1} became stronger. These losses vanished (with the exception of the 520 cm^{-1} loss) when the adsorbed layer was warmed to 420 K.

3.2. *Reactions of C_2H_5I and C_2H_5 Species*

As indicated by the XPS measurements the uptake of C_2H_5I on Rh(111) is only slightly affected by preadsorbed oxygen at $\Theta_O = 0.4$ (Fig. 1B). The position of the binding energy of I($3d_{5/2}$) remained practically constant at 619.7 eV for different exposures.

Annealing the coadsorbed layer resulted in a reduction of the intensity of the I peak above 225 K, where the binding energy of adsorbed I started shifting to lower energy. A constant value, 619.2 eV, was attained at 275–300 K (Fig. 5A). This is in contrast with the clean surface, where this shift began already at 150 K, and was complete at 225 K (Fig. 5B) (13).

TABLE 1

Vibrational Frequencies of CH_3I, CH_3, and CH_3O on Clean Rh(111) (cm^{-1})

Mode	CH_3I/Rh(111)[a]	CH_3/Rh(111)[a]	CH_3O/Rh(111)[b]
$\nu_a(CH_3)$		2920	
ν(C–H)			2935
$\nu_s(CH_3)$	3044		
δ(C–H)			1450
$\delta_a(CH_3)$	1430	1350	
ρ(C–H)			1130
$\delta_s(CH_3)$	1230	1185	
$\rho(CH_3)$	900	760	
ν(CO)			1015
δ(M–O–CH_3)			645
ν(C–I)	552		
ν(M–OCH_3)			345

[a] Reference (11).
[b] Reference (20).

TPD measurements showed that the product formation sensitively depends on the oxygen coverage. Detailed experiments have been performed at $\Theta_O = 0.3$, where the products of the oxidation reaction exhibited a maximum. Whereas C_2H_5I desorbs in two peaks ($T_p = 140$ K, denoted by α, and $T_p = 160$ K, denoted by β) from a clean Rh(111) surface, two additional peaks ($T_p = 200$ and 300 K, denoted by γ and δ) were observed for the oxygen-dosed surface (Fig. 6). Another important change is that the α peak ascribed to a multilayer became more dominant. The characteristics of the formation of products of C_2H_5 reaction on a clean surface also changed. The peak temperature of ethylene shifted from 220 to 300 K, and that of ethane from 168 to 230 K. The amount of ethylene produced was a factor of two higher and that of ethane a factor of two lower than on the clean surface. In the calculation of these values we took into account the sensitivity of our mass spectrometer to these compounds as well as their fragmentation patterns.

As the products of oxidation, H_2O, CO_2, and small amounts of CH_3CHO and CO were identified. Characteristic peak temperatures for the desorption of these products are as follows: $T_p(CH_3CHO) = 340$ K, $T_p(H_2O) = 320$ and 420 K, $T_p(CO_2) = 450$ and 500 K, $T_p(CO) = 500$ K. Taking into account the sensitivity of the mass spectrometer to the desorbing products, we calculated that about 70% of the C_2H_5 formed in the dissociation has been oxidized and the rest has been converted into ethylene and ethane.

Surface reactions occurring in the adsorbed layer have also been followed by HREELS measurements. Some spectra are shown in Fig. 7. The losses observed for oxygen-dosed Rh(111) at 95–300 K correspond well to those attributed to molecularly adsorbed C_2H_5I. New loss is seen in the CO stretching region at 2040–2050 cm^{-1} at and above

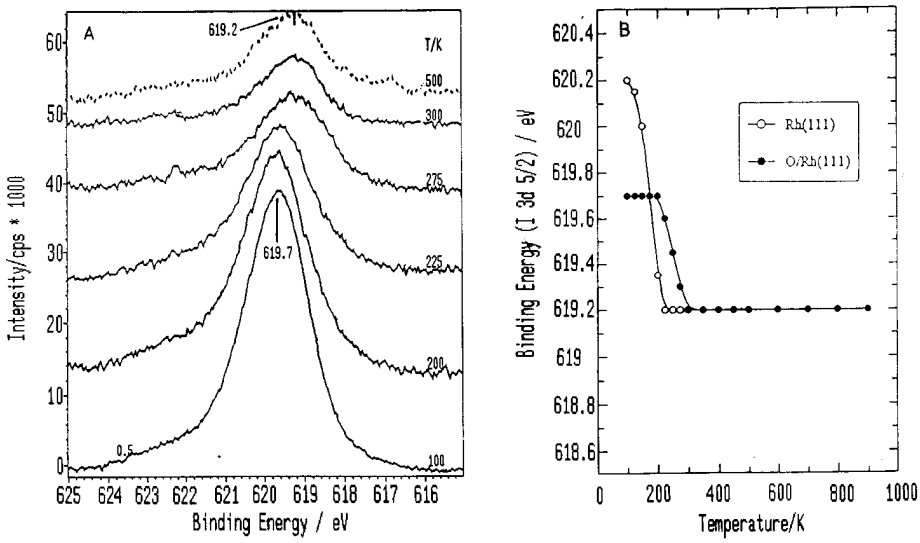

FIG. 5. (A) Effects of annealing on the XP spectra of adsorbed C_2H_5I on oxygen-dosed Rh(111) ($\Theta_O = 0.4$) and (B) on the position of I($3d_{5/2}$) peak. The exposure time of $C_2H_5I$was 8 min.

270 K. No other losses indicative of oxygen-containing species can be identified. Characteristic losses of adsorbed C_2H_5I, C_2H_5, and some oxygenated C_2-compounds on Rh(111) are presented in Table 2.

4. DISCUSSION

4.1. Chemistry of CH_3I on Oxygen-Dosed Rh(111)

XPS measurements indicate that the uptake of CH_3I on oxygen-saturated Rh(111) is only slightly altered as compared to the clean surface. The bonding of CH_3I, however, is strongly influenced by preadsorbed oxygen. In the XP spectra, a shift in the binding energy of I($3d_{5/2}$), corresponding to the dissociation of adsorbed CH_3I, occurred at higher temperatures than on a clean surface (Fig. 2). In accord with this, the vibration losses due to molecularly adsorbed CH_3I were eliminated at significantly higher temperatures, above 270 K, on oxygen-covered surfaces (Fig. 4). The higher stability of adsorbed CH_3I is also exhibited by the two new adsorption states, which are characterized by desorption peaks with $T_p = 180$ and 320 K. In the explanation of these new features we may assume that preadsorbed oxygen atoms, by occupying the adsorption sites, prevent the dissociation of CH_3I, and hence force a fraction of adsorbed molecules to desorb instead of dissociating. Some electronic effect may also operate.

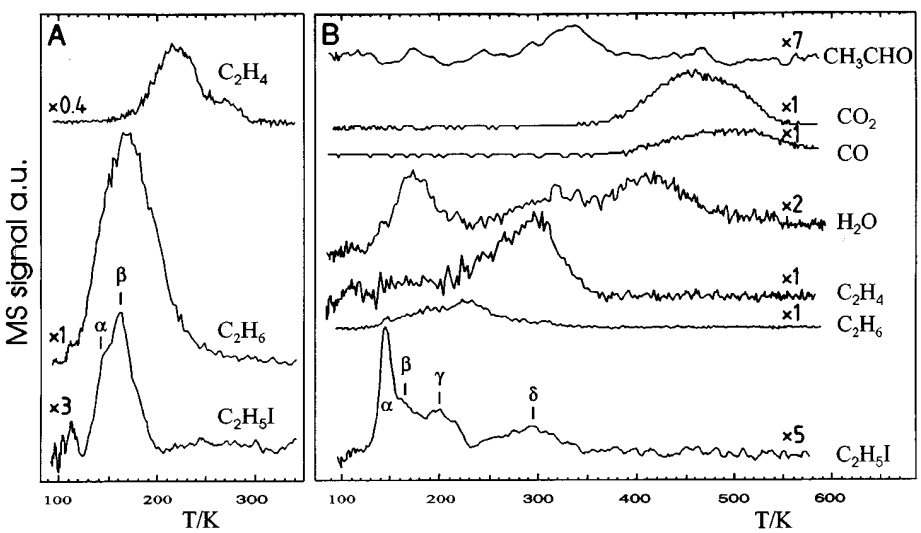

FIG. 6. TPD profiles of various products following C_2H_5I adsorption at 90 K on (A) clean and (B) oxygen-dosed Rh(111) at $\Theta_O = 0.3$. The exposure time of C_2H_5I was 4 min.

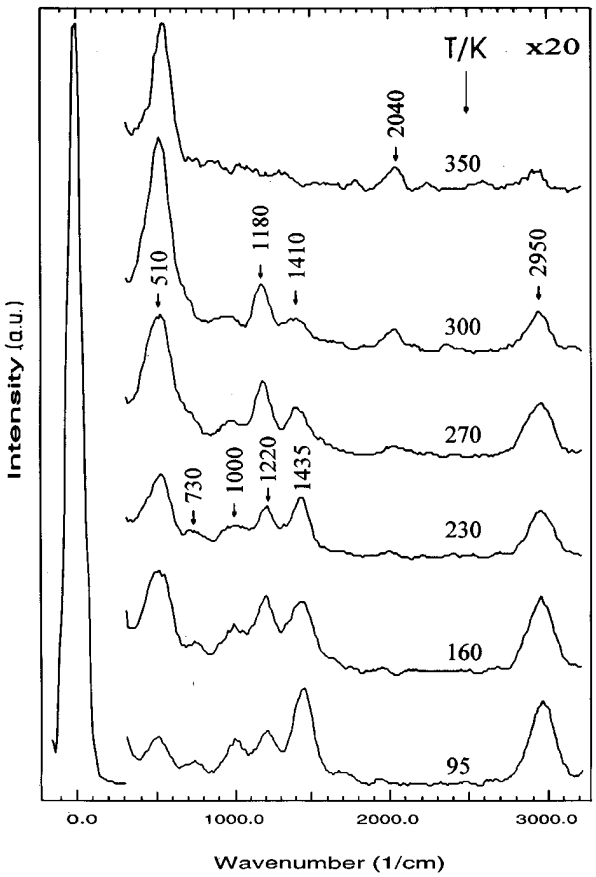

FIG. 7. HREEL spectra of adsorbed C_2H_5I on oxygen-covered Rh(111) ($\Theta_O = 0.4$) after annealing at different temperatures. The exposure time of C_2H_5I was 4 min.

4.2. Reactions of Adsorbed CH_3

The effect of preadsorbed oxygen is also manifested in the reactions of CH_3 observed for the clean surface: its self-hydrogenation into methane occurred in a wider temperature range than on the oxygen-free surface, and a significant portion of methane evolved only above 200 K. This suggests a certain stabilization of CH_3 species. In addition, a large fraction of CH_3 formed in the dissociation of CH_3I undergoes oxidation in the adsorbed layer at higher temperatures to produce H_2O, CO, and CO_2.

The obvious first step in the oxidation reaction is the selective addition of oxygen atoms to adsorbed CH_3 to yield methoxy species

$$CH_3(a) + O(a) = CH_3O(a),$$

similarly to the case of the $CH_2 + O$/Rh(111) system (12, 14). In the HREEL spectra, however, we found only a very weak loss at 1040–1050 cm^{-1} which can be attributed to the C–O stretch in methoxy species (Table 1) (20). This loss appeared at 150–180 K but was not discernible above 180 K. The weak signal of methoxy species may be associated with

TABLE 2

Vibrational Frequencies of C_2H_5I, C_2H_5, C_2H_5O, and CH_3CHO on Clean Rh(111) (cm^{-1})

Mode	$C_2H_5I_{(a)}$[a]	$C_2H_{5(a)}$[a]	$C_2H_5O_{(a)}$[b]	$CH_3CHO_{(a)}$[b]
ν(C–H)	2950	2910–2930	2990	2980
ν(C=O)				1460
$\delta(CH_3)$	1435	1420	1390	1380
$\delta(CH_2)$			1405	
$\omega(CH_2)$	1236	1150–1180		
ν_a(C–C–O)			1070	
ν_s(C–C–O)			880	
ν(C–C)	1000	940		1135
$\rho(CH_3)$		850		950
$\rho(CH_2)$	760			
δ (C–C–O)			510	610
ν(C–I)	516			
ν(M–C)		395		
ν(M–O)			nr	

[a] This work. Values shown represent average values of several experiments.
[b] Reference (29).

the fact that at 150–180 K we can expect only a very limited dissociation of adsorbed CH_3I.

The fact that the feature at 1040–1050 cm^{-1} was not detectable in the high-temperature region (where the dissociation of CH_3I is more extended) is not in contradiction with this picture, when we take into account the low stability of methoxy species on the Rh(111) surface (20–22). Following the adsorption of CH_3OH on clean Rh(111), where the surface concentration of methoxy species was obviously high, the losses due to methoxy species were identified only up to 180 K (20).

The difficulty of the formation of methoxy species in this system is consistent with the recent results of Friend (23), who found surface methoxy on Rh(111) only when adsorbed oxygen atoms were reacted with gaseous methyl radicals. No methoxy was detected in the reaction of adsorbed methyl and oxygen atoms (23). In the light of this finding the interaction of the CH_3 group of CH_3I should precede the formation of methoxy species. In other words, only those methyl groups of the adsorbed CH_3I molecules can produce methoxy species which interact with adsorbed oxygen atoms before the dissociation. Accordingly, the oxidation of CH_3 species is described in Scheme 1. The interaction of

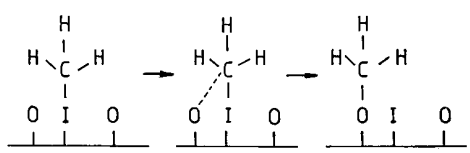

SCHEME 1

CH_3I with surface oxygen to yield methoxy is not unique, as it was also observed following the adsorption of CH_3I on Al_2O_3 (24).

The fact that the peak temperatures of the production of H_2O, CO, and CO_2 in the present case approach those measured following the adsorption of CH_3OH on oxygen-dosed Rh(111) (22) ($T_p(H_2O) = 375$ K, $T_p(CO) = 510$ K, $T_p(CO_2) = 450$ K) provides further evidence that the oxidation of CH_3 occurs through the transient formation and reactions of methoxy species. These reactions may involve the decomposition of CH_3O,

$$CH_3O(a) = CO(a) + 3H(a),$$

and the oxidation of adsorbed CO and H, and/or the direct oxidation of CH_3O to H_2O and CO_2. In the study of the reactions of CH_3O species on oxygen-dosed Rh(111) we came to the conclusion that the oxidation of adsorbed CO and H formed is the dominant pathway in the evolution of CO_2 and H_2O (22). Note that following the adsorption of CO_2 and H_2O on a Rh(111) surface, CO_2 desorbed with $T_p = 250$ K (25) and H_2O did so with $T_p = 158$ and 185 K (26).

In the above considerations several arguments have been presented to explain the low intensity of methoxy at low temperatures and its absence at high temperatures. An alternative interpretation is that the above route represents only a minor pathway in the oxidation of CH_3 species: the dominant process is the direct abstraction of hydrogens of CH_3 by adsorbed oxygen to give initially adsorbed OH and surface C. The oxidation of surface carbon on Rh, however, proceeds only above 550–600 K (27, 28). The peak temperatures of the CO evolution on Rh(111) are 660 and 750 K (28), which are considerably higher values than those determined for the production of CO and CO_2 in the present study. This makes the alternative route of the oxidation less likely.

4.3. Chemistry of C_2H_5 on Oxygen-Dosed Rh(111)

The uptake of C_2H_5I on oxygen-dosed Rh(111) did not change even at the highest oxygen coverage compared to the clean surface. As with CH_3I, preadsorbed oxygen markedly stabilized the molecularly adsorbed C_2H_5I towards dissociation. A detectable shift in the binding energy of I($3d_{5/2}$) occurred at temperatures about 75 K higher than those measured for the clean surface. The amount of desorbing C_2H_5I also increased, and two new adsorption states were produced. These features can be attributed to the blocking of the active surface sites for the dissociation of C_2H_5I, as discussed above.

4.4. Reactions of Adsorbed C_2H_5

In the case of a clean surface, C_2H_5 formed in the dissociation of C_2H_5I undergoes dehydrogenation to yield ethylene on the one hand and hydrogenates to C_2H_6 on the other hand (13). These reactions occurred in the presence of preadsorbed oxygen too. The formation of both ethylene and ethane, however, shifted to higher temperatures, very probably due to the delayed dissociation. In addition, the amount of ethane significantly decreased. The possible reason is that the hydrogen formed in the dehydrogenation of C_2H_5 reacted with adsorbed oxygen atoms to give H_2O. The release of H_2O at 260–360 K can be attributed to this process.

The oxidation of the C_2H_5 species also occurred in the adsorbed layer, as indicated by the formation of H_2O and CO_2 above 350–360 K, practically at the same temperature as in the case of CH_3 species.

We may assume that the oxidation of adsorbed ethyl proceeds in a similar way as described for the oxidation of adsorbed methyl species, i.e., through the interaction of the C_2H_5 group of adsorbed C_2H_5I with oxygen atoms and the transient formation and reactions of adsorbed ethoxy species. The fact that the ethoxy intermediate did not accumulate on the surface in a detectable amount at the temperature of the oxidation reaction is probably associated with its low thermal stability. Adsorbed C_2H_5O decomposes completely on Rh(111) to H and CO below 250 K (29). The formation of acetaldehyde may occur via β-hydrogen elimination of adsorbed ethoxy, as was established by Houtman and Barteau (29).

5. CONCLUSIONS

(i) The uptake of iodo compounds CH_3I and C_2H_5I at 95 K was not influenced by adsorbed oxygen up to $\Theta_O = 0.4$.

(ii) Adsorbed oxygen atoms, by occupying the active surface sites on the Rh surface, inhibit the dissociation of both CH_3I and C_2H_5I and induce the desorption of a fraction of strongly adsorbed CH_3I and C_2H_5I.

(iii) A weak electron energy loss signal at 1040–1050 cm^{-1} attributed to the C–O stretch in methoxy species has been identified at 150–180 K in the $CH_3I + O$/Rh(111) system.

(iv) Above 350 K the oxidation of adsorbed CH_3 and C_2H_5 starts to yield H_2O, CO, and CO_2. The product distributions depend on the oxygen concentration. At high oxygen coverage a small amount of gaseous acetaldehyde was observed in the oxidation of adsorbed ethyl species.

ACKNOWLEDGMENT

This work was supported by the Hungarian Academy of Sciences through Grant OTKA 95700.

REFERENCES

1. Poels, E. K., and Ponec, V., *in* "Catalysis," Specialist Periodical Report, Vol. 6, p. 196. Royal Society of Chemistry, London, 1983.
2. Solymosi, F., Tombácz, I., and Kocsis, M., *J. Catal.* **75**, 78 (1982).
3. Keim, W. D., Ed., "Catalysis in C_1 Chemistry." Reidel, Dordrecht, 1983.
4. Solymosi, F., Erdöhelyi, A., and Bánsági, T., *J. Catal.* **68**, 471 (1981).

5. Ramaroson, E., Kieffer, R., and Kiennemann, A., *J. Chim. Phys.* **79**, 749 (1987).
6. Richardson, J. T., and Paripatyadar, S. A., *Appl. Catal.* **61**, 293 (1990).
7. Solymosi, F., Kutsán, Gy., and Erdöhelyi, A., *Catal. Lett.* **11**, 149 (1991).
8. Erdöhelyi, A., Cserényi, J., and Solymosi, F., *J. Catal.* **141**, 287 (1993).
9. Solymosi, F., Erdöhelyi, A., Cserényi, J., *Catal. Lett.* **16**, 399 (1992); Solymosi, F., Erdöhelyi, A., Cserényi, J., and Felvégi,*J. Catal.* **147**, 272 (1994).
10. Solymosi, F., and Cserényi, J., *Catal. Lett.* **34**, 343 (1995).
11. Solymosi, F., and Klivényi, G., *J. Electron Spectrosc.* **64/65**, 499 (1993).
12. Klivényi, G., and Solymosi, F., *Surf. Sci.* **342**, 168 (1995).
13. Bugyi, L., Oszkó, A., and Solymosi, F., *Langmuit,* in press.
14. Solymosi, F., and Klivényi, G., *J. Phys. Chem.* **99**, 8950 (1995).
15. Wong, P. C., Hui, K. C., Zhou, M. Y., and Mitchell, K. A. R., *Surf. Sci.* **16**, L 21 (1986).
16. Xu, X., and Friend, C. M., *J. Am. Chem. Soc.* **113**, 6779 (1991).
17. Zhou, X.-L., Solymosi, F., Blass, P. M., Cannon, K. C., and White, J. M., *Surf. Sci.* **219**, 47 (1987).
18. Zaera, F., *J. Mol. Cat.* **86**, 221 (1994), and references therein.
19. Kovács, I., and Solymosi, F., *J. Phys. Chem.* **97**, 11056 (1993), and references therein.
20. Houtman, C., and Barteau, M. A., *Langmuir* **6**, 1558 (1990).
21. Solymosi, F., Berkó, A., and Tarnóczi, T. I., *Surf. Sci.* **141**, 533 (1984).
22. Solymosi, F., Tarnóczi, T. I., and Berkó, A., *J. Phys. Chem.* **88**, 6170 (1984).
23. Friend, C. M., private communication. (Paper presented at the IUVSTA workshop on "The Structure and Reactivity of Small Molecules on Surfaces," Brdo., April 9–15, 1995). Bol, C. W. Y., and Friend, C. M., J. Am. Chem. Soc. in press.
24. Beebe, T. P., Crowell, J. L., and Yates, J. T., Jr., *J. Phys. Chem.* **92**, 1296 (1988).
25. Kiss, J., Révész, K., and Solymosi, F., *Surf. Sci.* **207**, 36 (1988).
26. Kiss, J., and Solymosi, S., *Surf. Sci.* **177**, 191 (1986).
27. Sexton, B. A., and Somorjai, G. A., *J. Catal.* **46**, 167 (1978).
28. Kiss, J., Klivényi, G., Révész, K., and Solymosi, F., *Surf. Sci.* **223**, 5551 (1989).
29. Houtman, C. J., and Barteau, M. A., *J. Catal.* **130**, 528 (1991).